IMAGING

Single-cell bioluminescence imaging of deep tissue in freely moving animals

Satoshi Iwano,[1] Mayu Sugiyama,[1] Hiroshi Hama,[1] Akiya Watakabe,[2] Naomi Hasegawa,[2] Takahiro Kuchimaru,[3] Kazumasa Z. Tanaka,[4] Megumu Takahashi,[5] Yoko Ishida,[5] Junichi Hata,[6] Satoshi Shimozono,[1] Kana Namiki,[1] Takashi Fukano,[1] Masahiro Kiyama,[7] Hideyuki Okano,[6] Shinae Kizaka-Kondoh,[3] Thomas J. McHugh,[4] Tetsuo Yamamori,[2] Hiroyuki Hioki,[5] Shojiro Maki,[7] Atsushi Miyawaki[1,8]*

Bioluminescence is a natural light source based on luciferase catalysis of its substrate luciferin. We performed directed evolution on firefly luciferase using a red-shifted and highly deliverable luciferin analog to establish AkaBLI, an all-engineered bioluminescence in vivo imaging system. AkaBLI produced emissions in vivo that were brighter by a factor of 100 to 1000 than conventional systems, allowing noninvasive visualization of single cells deep inside freely moving animals. Single tumorigenic cells trapped in the mouse lung vasculature could be visualized. In the mouse brain, genetic labeling with neural activity sensors allowed tracking of small clusters of hippocampal neurons activated by novel environments. In a marmoset, we recorded video-rate bioluminescence from neurons in the striatum, a deep brain area, for more than 1 year. AkaBLI is therefore a bioengineered light source to spur unprecedented scientific, medical, and industrial applications.

Bioluminescence imaging (BLI) is based on the detection of light produced by the enzyme (luciferase)–catalyzed oxidation reaction of a substrate (luciferin) (*1*, *2*). In vivo BLI is a noninvasive method for measuring light output from luciferase-expressing cells after luciferin administration in living animals (*3*), and this method typically employs firefly luciferase (Fluc) and the natural substrate D-luciferin (Fig. 1A, left) that produces longer-wavelength (green-yellow) light and is more stable for enzymatic reaction after administration than the other commonly used luciferase substrate, coelenterazine (*4*–*7*). However, due to its relatively low tissue permeability, D-luciferin has a heterogeneous biodistribution in the body (*8*). The low affinity (high Michaelis constant, K_M) of D-luciferin for Fluc also suggests uneven saturation of the Fluc reporter enzyme with substrate in vivo. In particular, in vivo BLI in the brain has been hampered due to low passage of D-luciferin through the blood-brain barrier (BBB) (*8*). In recent years, synthetic analogs of D-luciferin were reported (*9*–*11*), including AkaLumine (Fig. 1A, right), that when catalyzed by Fluc produces near-infrared emission peaking at 677 nm, which can penetrate most animal tissues and bodies. We previously demonstrated that AkaLumine hydrochloride (AkaLumine-HCl) has favorable biodistribution to access Fluc-expressing cells in deep organs such as the lung and can saturate Fluc more effectively than D-luciferin (*12*).

We hypothesized that Fluc is not enzymatically optimal for AkaLumine-HCl; therefore, we performed directed evolution on the luciferase gene through successive rounds of mutagenesis, screening, and validation to develop an enzyme that could strongly pair with AkaLumine-HCl. We constructed gene libraries encoding variants of three luciferases (*13*)—Fluc, emerald luciferase (Eluc), and crick beetle red luciferase (CBRluc)—and screened them by selecting for bacterial colonies with brighter emission in the presence of AkaLumine (fig. S1A). Candidates in the Fluc-based library were iteratively screened with multiple cycles of random mutagenesis (fig. S1B) to produce Akaluc, which has 28 amino acid substitutions relative to Fluc (fig. S1C). Application of D-luciferin and AkaLumine on bacterial colonies expressing Akaluc or Fluc enabled bright near-infrared emission with AkaLumine/Akaluc and very weak emission with the other combinations (fig. S2). In vitro experiments with purified luciferases (Fig. 1B) showed that Akaluc catalyzed AkaLumine ~7 times more efficiently than Fluc to produce emissions with a maximum at 650 nm (fig. S3). Their catalytic activity was equally pH-sensitive (fig. S4) and, in addition, Akaluc exhibited higher thermostability than Fluc (fig. S5).

Akaluc-expressing HeLa cells (HeLa/Akaluc cells) were constructed after transfection with a cDNA encoding Venus-Akaluc and purification by flow cytometry for Venus fluorescence. Likewise, HeLa/Fluc cells were also prepared. We examined the comparative BLI performance of the four luciferin/luciferase combinations (Fig. 1C). To compare the performance of Akaluc and Fluc for AkaLumine in cultured cells, we additionally performed a comparative experiment using HeLa/Akaluc cells and HeLa/Fluc cells exposed to 500 μM AkaLumine (fig. S6A). The cellular BLI signal ratio of Venus-Akaluc to Venus-Fluc was ~52. In addition, we analyzed Venus-luciferase–expressing HeLa cells by flow cytometry and quantified the expression level ratio of Venus-Akaluc to Venus-Fluc to be ~4. Accordingly, we assigned the ~13-fold improvement of Akaluc over Fluc to an improvement intrinsic to luciferase's catalytic activity. Akaluc showed a 3.79 ± 0.20 (n = 58) times higher expression level compared with Fluc (fig. S6B) despite the same speed of folding/degradation (fig. S7). Based on these results, we conclude that in cultured cells, Akaluc performs better than Fluc due to a 7- to 13-fold enhancement of its catalytic activity and a roughly 4-fold improvement in the expression level.

We next compared the in vivo BLI performance of AkaLumine-HCl/Akaluc and D-luciferin/Fluc in deep tissues of mice. Whereas in vitro and cellular BLI employs AkaLumine, in vivo BLI uses AkaLumine-HCl (see the supplementary materials). Care was taken in this study regarding the route, timing, and dose of systemic administration of the substrates (fig. S8). Considering the high K_M value for Fluc and the poor tissue delivery of D-luciferin, a relatively high dose of the substrate was injected (500 nmol/g body weight, comparable to a 100 μl volume of 100 mM D-luciferin for an average-sized mouse). In contrast, a 100 μl solution of 30 mM AkaLumine-HCl was injected into mice, a dose previously shown to provide a saturating concentration in vivo of AkaLumine-HCl (*12*).

We localized luciferase expression deep inside the mouse body by two approaches, (i) cell implantation in the vasculature and (ii) viral transduction in the brain. In the former approach, HeLa/Akaluc or HeLa/Fluc cells were transplanted. We injected 10^3 cells into the tail vein. Using this protocol, the majority of intravenously injected cells are initially trapped in the small capillaries of the lung (*14*, *15*); thus, we imaged the upper part of an anesthetized animal 10 min after cell injection and immediately after intraperitoneal substrate administration. Under these conditions, the AkaLumine-HCl/Akaluc combination yielded a 52 ± 9.5-fold stronger signal than D-luciferin/Fluc (Fig. 1D).

[1]Laboratory for Cell Function and Dynamics, Brain Science Institute, RIKEN, 2-1 Hirosawa, Wako-city, Saitama 351-0198, Japan. [2]Laboratory for Molecular Analysis of Higher Brain Function, Brain Science Institute, RIKEN, 2-1 Hirosawa, Wako-city, Saitama 351-0198, Japan. [3]School of Life Science and Technology, Tokyo Institute of Technology, 4259 Nagatsuta, Midori-ku, Yokohama 226-8501, Japan. [4]Laboratory for Circuit and Behavioral Physiology, Brain Science Institute, RIKEN, 2-1 Hirosawa, Wako-city, Saitama 351-0198, Japan. [5]Department of Morphological Brain Science, Graduate School of Medicine, Kyoto University, Yoshida-Konoe-Cho, Sakyo-ku, Kyoto 606-8501, Japan. [6]Laboratory for Marmoset Neural Architecture, Brain Science Institute, RIKEN, 2-1 Hirosawa, Wako-city, Saitama 351-0198, Japan. [7]Graduate School of Informatics and Engineering, The University of Electro-Communications, 1-5-1 Chofugaoka, Chofu-city, Tokyo 182-8585, Japan. [8]Biotechnological Optics Research Team, Center for Advanced Photonics, RIKEN, 2-1 Hirosawa, Wako-city, Satitama 351-0198, Japan.
*Corresponding author. Email: matsushi@brain.riken.jp

In the second approach, we imaged bioluminescence from the striatum, a group of contiguous subcortical structures deep in the brain involved in motor control and other functions. Because access of D-luciferin to the brain is limited by the BBB (*8*) but AkaLumine-HCl is tissue-permeant (*12*), we expected that brain imaging should benefit from AkaLumine-HCl/Akaluc. We used an adeno-associated virus (AAV)–based tetracycline (TET)–inducible system (*16*) for expression of Akaluc or Fluc (fig. S9) in the striatum. Two weeks after viral infection, mouse heads were comparatively imaged after substrate administration (intraperitoneal). First, the activity of striatally expressed Fluc was examined with different substrates, indicating that AkaLumine-HCl was more accessible to the brain than another reported synthetic analog CycLuc1 (*10*), as well as D-luciferin (fig. S10). In a pair of mice, strong and faint bioluminescence signals were observed for the AkaLumine-HCl/Akaluc and D-luciferin/Fluc combinations, respectively (Fig. 1E, top). We verified that a 100-μl solution of 30-mM AkaLumine-HCl was sufficient for saturating striatally expressed Akaluc (fig. S11) and that both the AkaLumine-HCl/Akaluc and D-luciferin/Fluc signals developed in a similar sustained pattern, peaking around 10 to 20 min after substrate administration (intraperitoneal) (fig. S12). Statistical analysis revealed that AkaLumine-HCl/Akaluc yielded a 1408 ± 375-fold stronger signal than D-luciferin/Fluc (Fig. 1E, middle, fig. S10), which is a more prominent improvement than that observed for pulmonary localization (Fig. 1D).

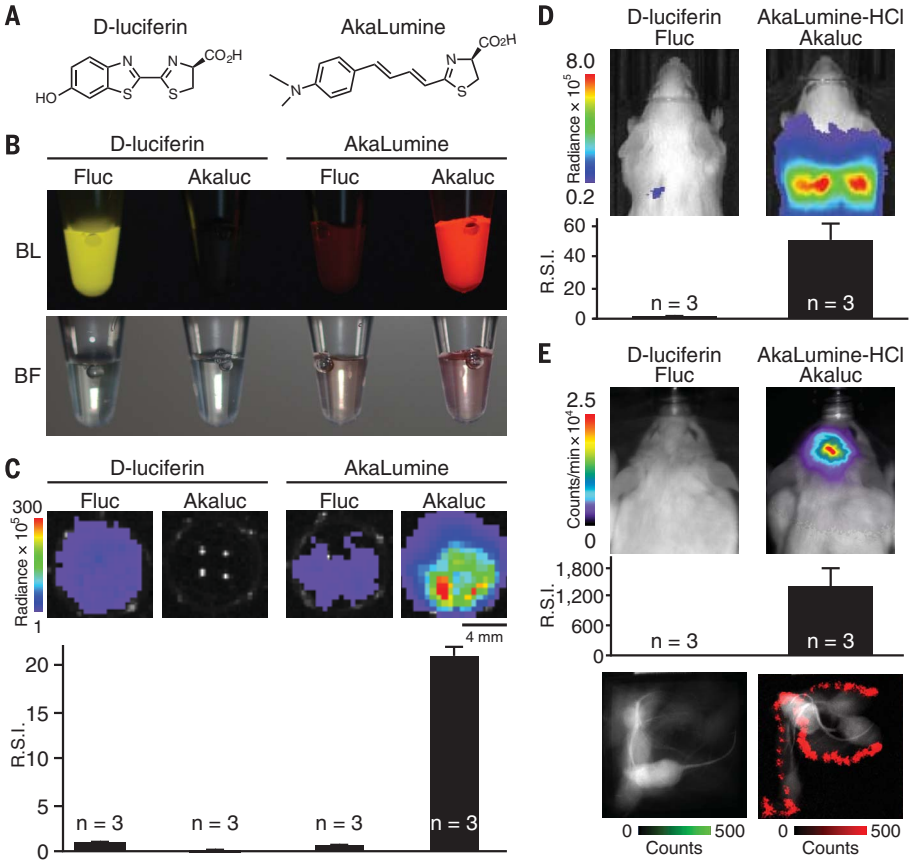

Fig. 1. Performance of engineered AkaLumine/Akaluc versus natural D-luciferin/Fluc for in vitro and in vivo bioluminescence imaging. (**A**) Chemical structures of D-luciferin (left) and AkaLumine (right). (**B**) BLI of four mixtures of the substrate (100 μM) and enzyme (2 mg/ml). Color images of solutions containing (from left to right) D-luciferin/Fluc, D-luciferin/Akaluc, AkaLumine/Fluc, and AkaLumine/Akaluc. BL, bioluminescence (top). BF, bright-field (bottom). (**C**) Comparative BLI of cultured cells with the four substrate/enzyme combinations described in (B). HeLa cells expressing Fluc or Akaluc were treated with 250 μM D-luciferin (left) or 250 μM AkaLumine (right) and imaged using a cooled charge-coupled device (CCD) camera (1-min exposure time). Similar results were obtained from two other experiments. Bioluminescence signals were quantified and normalized to that of the D-luciferin/Fluc system. Data are presented as mean ± SEM of three independent experiments. (**D**) Bioluminescence images of mice intravenously injected with 10^3 HeLa cells expressing Fluc (left) or Akaluc (right). Substrate administration was performed intraperitoneally. Images were acquired using a cooled CCD camera (1-min exposure time). The AkaLumine-HCl/Akaluc signals were statistically compared to D-luciferin/Fluc signals. Data are presented as mean ± SEM of $n = 3$ mice. (**E**) Bioluminescence images of mice 2 weeks after viral infection for expression of Fluc (left) and Akaluc (right) in the right striatum. Immediately after substrate administration (intraperitoneal), anesthetized mice were imaged using a cooled CCD camera (top). The AkaLumine-HCl/Akaluc signals were statistically compared to D-luciferin/Fluc signals (middle). Data are presented as mean ± SEM of $n = 3$ mice. After intravenous injection with their respective substrates, mice were allowed to behave naturally in the arena (bottom). Bioluminescence and bright-field images (30-msec exposure time for each) were alternately acquired using an electron-multiplying CCD (EM-CCD) camera. An integrated image spanning 5 s is shown. Bioluminescence signals are shown in green (D-luciferin/Fluc) and red (AkaLumine-HCl/Akaluc). Bright-field signals are shown in black and white. Mice were injected with 100 to 200 μl of D-luciferin (100 mM) or AkaLumine-HCl (30 mM) [(D) and (E)]. The color bars indicate the total bioluminescence radiance (photons/sec/cm^2/sr) [(C) and (D)] and counts/min (E). R.S.I., relative signal intensity [(C) to (E)].

The all-engineered BLI system composed of AkaLumine-HCl and Akaluc is hereafter referred to as AkaBLI. AkaBLI with intravenous administration allowed the monitoring of brain striatal bioluminescence at video rate in a freely moving mouse for >1 hour (Fig. 1E, bottom right; fig. S13; and movie S1), demonstrating the practical applicability of AkaBLI for studying naturally behaving animals. The same measurement was not possible with D-luciferin/Fluc (Fig. 1E, bottom left). We also monitored the signal development of striatal AkaBLI via three major systemic administration routes (fig. S8). We found that the maximal intensity was higher in the order of intravenous, intraperitoneal, and oral administration and that intravenous gave the same temporal profile as intraperitoneal, whereas oral gave the most persistent bioluminescence (fig. S14). In a trial experiment, after 1 day of water deprivation we gave the mouse ad libitum oral access to an AkaLumine-HCl solution and recorded striatal AkaBLI. About 5 min after several fluid intakes, a substantial amount of bioluminescence became apparent on the head and was monitored at video rate for more than 1 hour (fig. S15 and movie S2). Such painless and voluntary self-administration of substrate to awake animals will be useful for BLI experiments under natural conditions and to assess sensitive behavioral changes.

Based on the bright bioluminescence signals from HeLa/Akaluc cells in the mouse lung (Fig. 1D), we examined the cell sensitivity of AkaBLI as a quantitative method to examine pulmonary cell trapping by titrating down the number of injected HeLa/Akaluc cells. By observation of Venus fluorescence, we prepared solutions that contained 1, 2, 3, or 10 HeLa/Akaluc cells (fig. S16). Twelve mice were injected with a 1-cell–containing solution (nos. 1 to 12). A focal bioluminescent signal was observed over the upper back of mice 6 and 9 (Fig. 2, 1 cell), presumably derived from the one HeLa/Akaluc cell trapped

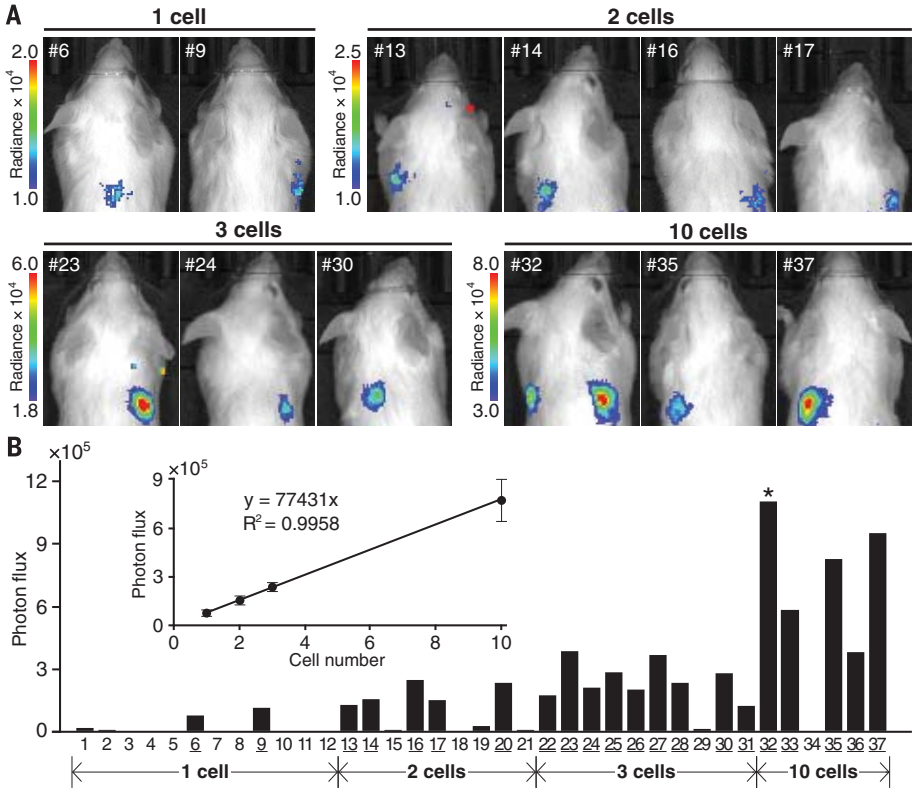

Fig. 2. Analysis of single-cell and sparse-cell AkaBLI of implanted tumorigenic cells trapped in the mouse lung. Detection (all-or-nothing) of bioluminescence from a small number of Akaluc-expressing HeLa cultured cells trapped in the mouse lung. An anesthetized mouse was intravenously injected with the indicated number of cells and 10 min later with 100 µl of AkaLumine-HCl (30 mM). Bioluminescence images were acquired using a cooled CCD camera (1-min exposure time). Mouse samples nos. 1 to 12, 13 to 21, 22 to 31, and 32 to 37 were injected with 1, 2, 3, and 10 cells, respectively. (**A**) Representative images with substantial bioluminescent signals. Mouse sample numbers are indicated inside. The color bars indicate the total bioluminescence radiance (photons/sec/cm^2/sr). (**B**) Bioluminescence was quantified for each mouse and plotted. Numbers of samples with a significant amount of signal are underlined. The bioluminescent signals (mean ± SEM) of the underlined samples are plotted as a function of cell number (inset).

in the lung. No signal was detected from the other 10 mice, suggesting efficient pulmonary passage of single cells. Likewise, mice injected with 2, 3, and 10 cells were imaged. Bioluminescence signals were observed in 5 of 9 mice given the 2-cell injection (Fig. 2, 2 cells) and in 9 of 10 mice given the 3-cell injection (Fig. 2, 3 cells), and all of them appeared as single foci. The 10-cell injection produced a focal fission in mouse 32 and single foci in mice 33, 35, 36, and 37 (Fig. 2, 10 cells). Because the bioluminescent foci mostly occurred singly on the body surface, and because the total bioluminescence intensity was linearly correlated with the number of injected cells (Fig. 2B, inset), it is likely that multiple circulating HeLa/Akaluc cells were clustered before being trapped in the lung. It is also noted that larger clusters were trapped in the lung more frequently; the bioluminescence detection rates were 2 of 12, 5 of 9, 9 of 10, and 5 of 6 for 1-, 2-, 3-, and 10-cell injections, respectively. This result agrees with a previous finding that pulmonary trapping depends on the size of infused cell clumps (*14*, *15*). Although single-cell transplantation of fluorescent protein–labeled bone marrow cells was previously performed (*17*, *18*), their repopulating activity was analyzed retrospectively by flow cytometry. In contrast, AkaBLI will allow real-time long-term monitoring of transplanted stem cells at the single-cell level.

We examined the capability of functional AkaBLI to detect behaviorally induced longitudinal changes in deep brain structures. We used neuronal-activity–dependent expression of immediate early genes (IEGs), including c-Fos and c-Arc, to genetically mark neurons responsible for encoding learned experiences (*19*–*21*). Previous studies identified neurons activated by experiences occurring within a limited time window before sacrifice using postmortem histological techniques for the detection of IEG expression in fixed tissue (*22*, *23*). Here, to noninvasively monitor active ensembles in the hippocampus during spatial learning and adaptation in a single living mouse, we designed an experimental system (Fig. 3A), in which Venus-Akaluc was expressed under the control of the *c-fos* promoter. The coupling between activity-dependent transcription and reporter gene expression was controlled by doxycycline (Dox) in the diet. A recombinant AAV expressing TRE-Venus-Akaluc was targeted unilaterally (right) to the CA1 area of hippocampus in a transgenic mouse line expressing c-fos-tTA (Fig. 3B). The experimental protocol using a single virus-infected mouse was composed of three consecutive observation epochs (1, 2, and 3) (Fig. 3C). In each epoch, three BLIs were carried out under anesthesia. The first BLI provided the background signal after Dox was withheld from the mouse for 48 hours (Fig. 3D, gray circles). Then, about 17 hours later, the mouse was allowed to explore a novel context (red cross) or a familiar context (blue cross) for 15 min × 2. Exactly 7 hours after the exploration, the second BLI gave an exploration-dependent change in the signal (Fig. 3D, red circles). Finally, the mouse was maintained on a Dox diet for a long time (>4 days) for the complete removal of TRE-Venus-Akaluc signal, which was confirmed by a background-level signal of the third BLI (Fig. 3D, black circles). These data serve as a practical indication of the sufficient degradation of the Akaluc reporter in multiple observations 1, 2, and 3, involving a novel environment, a return to the familiar home cage, and another novel environment, respectively (Fig. 3C). The temporal profile of the bioluminescence (Fig. 3D and fig. S17) validates the capability of AkaBLI to reliably track the response history of the same neurons to multiple stimuli over many days. Photographs of the first, second, and third BLIs during observation 1 (i, ii, and iii, respectively) (Fig. 3E) show the focal occurrence of the bioluminescence signal, indicating that the infection was confined to the injection site. About 8 hours after a treatment with kainic acid for the full activation of the infected neurons, we fixed the brain for tissue clarification with the Sca*l*eS technique (*24*) and focused on the region containing the cortex and hippocampus for a three-dimensional reconstruction of Venus-expressing neurons (Fig. 3, F and G). Unexpectedly, only 49 neurons were identified as fluorescent and presumed bioluminescent emitters (Fig. 3G). We statistically validated the novelty-dependent increase in the neuronal activation signals over the background (Fig. 3H) and home-cage signals (Fig. 3I). The results demonstrate that AkaBLI can be used to directly monitor the activation patterns of much fewer numbers of neurons than any existing noninvasive optical

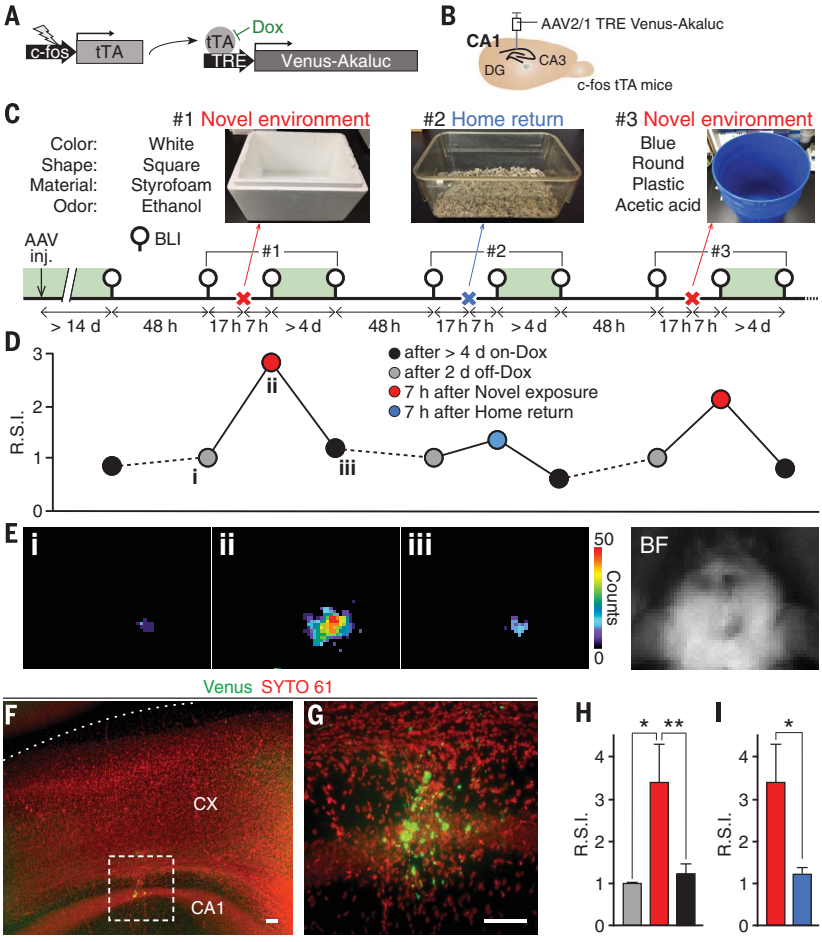

Fig. 3. Noninvasive monitoring of neuronal ensemble responses to novel environments in mouse hippocampal CA1 using AkaBLI. (**A** and **B**) c-fos-tTA mice were injected with AAV-TRE-Venus-Akaluc (A) targeting the right hippocampal CA1 region. (B) While off-Dox, exposure to a novel environment induces c-fos–dependent expression of tTA, which binds to the TRE and drives the expression of Venus-Akaluc, labeling a subpopulation of activated neurons. (**C**) Experimental setup to study brain responses to two novel environments: a white, square styrofoam box with an alcohol odor (#1), and a blue, round plastic bucket with an acetic acid odor (#3). The familiar context was a home cage (#2). Shown below is the experimental scheme containing three consecutive observation epochs: 1 to 3. BLI: Mice were anesthetized, administered (intraperitoneally) with AkaLumine-HCl (75 nmol/g body weight), and then imaged using a cooled CCD camera (5-min exposure time). Depilation was performed during the on-Dox period (green shade). (**D** and **E**) BLI data of a representative mouse, which showed a novel-context dependent increase in the bioluminescence signal. R.S.I., relative signal intensity. BLI time points correspond to BLI symbols shown in (C). Photographs of the first, second, and third BLIs during observation 1 [i, ii, and iii, respectively (D)] with bright-field image (BF) are shown (E). The color bar indicates the total bioluminescence counts/5 min. (**F** and **G**) Three-dimensional reconstructions of infected neurons with Venus expression (green) in a cleared brain sample stained for nucleic acid with SYTO 61 (red). Maximum projection images of the region containing the cortex (CX) and the hippocampal CA1. A magnified micrograph (G) (80-μm volume, 0.5-μm step size) corresponding to the box shown in (F) (910-μm volume, 6.1-μm step size). Scale bars, 100 μm. (**H** and **I**) Statistical analysis of BLI data. Bioluminescence signals after novel exposure (red) compared with those taken 1 day earlier (gray) and >4 day later with Dox (black) (H). Bioluminescence signals after novel exposure (red) compared with those after home cage return (blue) (I). Data are presented as mean ± SEM (n = 6 mice). *P < 0.05. **P < 0.01. Significance was calculated by means of two-sided paired t tests.

technique (*25*), therefore allowing the visualization of genetically defined small neural ensembles.

We examined AkaBLI as a method for the long-term noninvasive monitoring of the brain in a higher-order species by performing AkaBLI in the marmoset, a small New World monkey (*26*). A 4-year-old female marmoset was introduced with recombinant AAVs for expression of Akaluc. The injection was precisely guided by magnetic resonance imaging (MRI) (*27*) of the right striatum located 4.8 mm from the brain surface (Fig. 4A). The depilated head was imaged under anesthesia after AkaLumine-HCl administration (intraperitoneal), and AkaBLI was repeated every month at minimum. The bioluminescence emitted from the striatum was detected through the intact head, with an intensity peaking at 20 to 30 min after substrate administration (fig. S18). The BLI signal greatly increased over the 3 months after injection (Fig. 4B) and then lasted for many months (Fig. 4C), suggesting stable integration of the transgene in the transduced neurons. At 1 year after injection, we used a fast mode of BLI without anesthesia, and we were able to follow striatal bioluminescence with a 100-msec exposure time for over 1 hour while the 5-year-old female marmoset was freely moving (Fig. 4D, fig. S19, and movie S3). Her behavior was normal, suggesting that the dose of AkaLumine-HCl administration had no overt side effects (fig. S20). Such video-rate long-lasting and noninvasive BLI will have many applications in neuroscience for mapping and probing neural circuitry in behaving animals under natural conditions (*28*, *29*).

In this study, the directed evolution of firefly luciferase with an artificial substrate allowed a major improvement for in vivo deep bioluminescence imaging. The AkaBLI system, composed of AkaLumine-HCl and Akaluc, enabled the improved performance by optimized Akaluc yield and catalysis of AkaLumine-HCl compared with Fluc. In accord, AkaBLI displayed superior sensitivity for in vivo noninvasive BLI in long-lasting video-rate monitoring of a few cells in freely moving animals. Importantly, we chose to demonstrate the AkaBLI in deep tissue areas to highlight the strength of the light source to penetrate body walls while retaining accurate spatial and temporal specificity. In contrast, current coelenterazine-based BLI systems are useful in dissociated cell- and slice-based in vitro applications but do not have adequate substrate biodistribution in animals in vivo (*4*, *5*, *30*, *31*) (figs. S21 and S22), and there is no reliable evidence to date of the practical applicability of coelenterazine substrates for in vivo physiological studies. In contrast, AkaLumine-HCl has high permeability and stability for homogeneous substrate distribution inside the body, including the ability to cross the BBB into the brain. Thus, AkaBLI is expected to accurately map reporter enzyme expression as opposed to substrate distribution. Further coevolution of BLI enzymes and substrates will be a promising approach to synthetic biological light

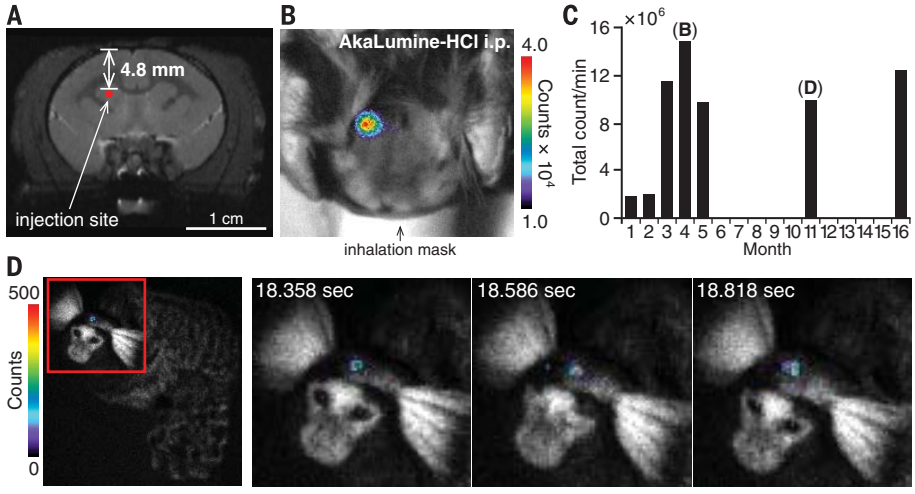

Fig. 4. Chronic video-rate AkaBLI of brain striatal neurons in a common marmoset. (**A**) Brain MRI picture (T2 weighted image) showing guided AAV injection into the right striatum of a 4-year-old female marmoset for expression of Venus-Akaluc. (**B**) A bioluminescence image 4 months after injection. After the AkaLumine-HCl (75 nmol/g body weight) administration (intraperitoneal), the head of the anesthetized marmoset was imaged using an EM-CCD camera (30-s exposure time). (**C**) Bioluminescence signals were quantified and plotted against time after injection. Due to growth with various degrees of depilation during the long time period, the efficiency of bioluminescence collection varied, and the data are displayed by a bar graph. (**D**) Bioluminescence images 12 months after injection. After AkaLumine-HCl administration (intraperitoneal), the entire marmoset (naturally behaving) was imaged using an EM-CCD camera (100-msec exposure time). An eye blink was recorded in three consecutive, expanded images. The color bars indicate the total bioluminescence counts/30 s (B) and counts/100 msec (D).

production for research, industry, and medical applications.

REFERENCES AND NOTES

1. T. Wilson, J. W. Hastings, *Annu. Rev. Cell Dev. Biol.* **14**, 197–230 (1998).
2. C. H. Contag, M. H. Bachmann, *Annu. Rev. Biomed. Eng.* **4**, 235–260 (2002).
3. A. Sacco, R. Doyonnas, P. Kraft, S. Vitorovic, H. M. Blau, *Nature* **456**, 502–506 (2008).
4. A. Pichler, J. L. Prior, D. Piwnica-Worms, *Proc. Natl. Acad. Sci. U.S.A.* **101**, 1702–1707 (2004).
5. N. Vassel *et al.*, *Luminescence* **27**, 234–241 (2012).
6. L. Mezzanotte *et al.*, *Contrast Media Mol. Imaging* **8**, 505–513 (2013).
7. A. C. Stacer *et al.*, *Mol. Imaging* **12**, 457–469 (2013).
8. K.-H. Lee *et al.*, *Nucl. Med. Commun.* **24**, 1003–1009 (2003).
9. S. Iwano *et al.*, *Tetrahedron* **69**, 3847–3856 (2013).
10. M. S. Evans *et al.*, *Nat. Methods* **11**, 393–395 (2014).
11. A. P. Jathoul, H. Grounds, J. C. Anderson, M. A. Pule, *Angew. Chem. Int. Ed. Engl.* **53**, 13059–13063 (2014).
12. T. Kuchimaru *et al.*, *Nat. Commun.* **7**, 11856 (2016).
13. Z. M. Kaskova, A. S. Tsarkova, I. V. Yampolsky, *Chem. Soc. Rev.* **45**, 6048–6077 (2016).
14. S. Schrepfer *et al.*, *Transplant. Proc.* **39**, 573–576 (2007).
15. U. M. Fischer *et al.*, *Stem Cells Dev.* **18**, 683–692 (2009).
16. J. Sohn *et al.*, *PLOS ONE* **12**, e0169611 (2017).
17. H. Ema *et al.*, *Dev. Cell* **8**, 907–914 (2005).
18. R. Yamamoto *et al.*, *Cell* **154**, 1112–1126 (2013).
19. L. G. Reijmers, B. L. Perkins, N. Matsuo, M. Mayford, *Science* **317**, 1230–1233 (2007).
20. S. Kubik, T. Miyashita, J. F. Guzowski, *Learn. Mem.* **14**, 758–770 (2007).
21. K. J. Kovács, *J. Neuroendocrinol.* **20**, 665–672 (2008).
22. C. J. Guenthner, K. Miyamichi, H. H. Yang, H. C. Heller, L. Luo, *Neuron* **78**, 773–784 (2013).
23. Y. Kim *et al.*, *Cell Reports* **10**, 292–305 (2015).
24. H. Hama *et al.*, *Nat. Neurosci.* **18**, 1518–1529 (2015).
25. M. Eguchi, S. Yamaguchi, *Neuroimage* **44**, 1274–1283 (2009).
26. K. Mansfield, *Comp. Med.* **53**, 383–392 (2003).
27. T. Hashikawa, R. Nakatomi, A. Iriki, *Neurosci. Res.* **93**, 116–127 (2015).
28. O. Sadakane *et al.*, *Cell Reports* **13**, 1989–1999 (2015).
29. H. Okano *et al.*, *Neuron* **92**, 582–590 (2016).
30. J. Chu *et al.*, *Nat. Biotechnol.* **34**, 760–767 (2016).
31. H.-W. Yeh *et al.*, *Nat. Methods* **14**, 971–974 (2017).

ACKNOWLEDGMENTS

The authors thank K. Ohtawa and R. Takahashi for technical assistance; S. Okabe for advice; Kurogane Kasei Co., Ltd., for providing AkaLumine and AkaLumine-HCl; Summit Pharmaceuticals International Corporation for granting the temporary use of IVIS Lumina III; and C. Yokoyama for manuscript editing. **Funding:** This work was supported in part by grants from the Japan Ministry of Education, Culture, Sports, Science, and Technology Grant-in-Aid for Scientific Research on Innovative Areas: Resonance Bio (15H05948 to A.M; 16H01426 to H. Hioki); Scientific Research (16H04663 to H. Hioki); Exploratory Research (17K19451 to H. Hioki; 24650633 to S.M.); Adaptive, Seamless Technology Transfer Program through target-driven R&D JST (AS2614119N to S.M); and the Brain Mapping by Integrated Neurotechnologies for Disease Studies (Brain/MINDS) and Japan Agency for Medical Research and Development-Core Research for Evolutional Science and Technology (AMED-CREST), the Uehara Memorial Foundation, and Special Postdoctoral Researchers Program from RIKEN (S.I.). **Author contributions:** S.I. and A.M. conceived and designed the whole study. S.I. performed all the experiments and analyzed the data. M.S. analyzed Fluc mutants in cultured cells. S.S. performed gene construction. H. Hama designed and performed histological experiments. K.N. acquired light-sheet microscopy images. T.F. studied the thermostability of luciferases. A.W., N.H., J.H., H.O., and T.Y. performed AkaBLI experiments with the marmoset. T.K. and S.K.-K. performed AkaBLI experiments of pulmonary trapping of transplanted tumor cells. M.T., Y.I., and H. Hioki prepared AAVs. K.Z.T., H. Hioki, and T.J.M designed AkaBLI experiments for observing novelty-dependent neuronal activation. M.K. and S.M. performed quantum yield measurement and diphenylterazine synthesis. A.M. wrote the manuscript and supervised the project. **Competing interests:** S.I. and A.M. are inventors on patent application PCT/JP2017/030491 submitted by RIKEN that covers the creation and use of Akaluc. **Data and materials availability:** The data reported in this paper are presented in the main text and supplemental materials. The Akaluc genes (pcDNA3/Venus-Akaluc, pAAV2 SynTetOff Venus-Akaluc, pAAV2 TRE Venus-Akaluc) will be available from the RIKEN Bio-Resource Center (BRC) (http://en.brc.riken.jp) under a material transfer agreement with RIKEN. The accession number in the DDBJ/EMBL/GenBank database is LC320664 for Akaluc.

SUPPLEMENTARY MATERIALS

www.sciencemag.org/content/359/6378/935/suppl/DC1
Materials and Methods
Figs. S1 to S22
Table S1
Movies S1 to S3
References (*32*–*39*)

3 October 2017; accepted 31 December 2017
10.1126/science.aaq1067

Science

Single-cell bioluminescence imaging of deep tissue in freely moving animals

Satoshi Iwano, Mayu Sugiyama, Hiroshi Hama, Akiya Watakabe, Naomi Hasegawa, Takahiro Kuchimaru, Kazumasa Z. Tanaka, Megumu Takahashi, Yoko Ishida, Junichi Hata, Satoshi Shimozono, Kana Namiki, Takashi Fukano, Masahiro Kiyama, Hideyuki Okano, Shinae Kizaka-Kondoh, Thomas J. McHugh, Tetsuo Yamamori, Hiroyuki Hioki, Shojiro Maki and Atsushi Miyawaki

Science **359** (6378), 935-939.
DOI: 10.1126/science.aaq1067

Improved spy tactics for single cells

Bioluminescence imaging is a tremendous asset to medical research, providing a way to monitor living cells noninvasively within their natural environments. Advances in imaging methods allow researchers to measure tumor growth, visualize developmental processes, and track cell-cell interactions. Yet technical limitations exist, and it is difficult to image deep tissues or detect low cell numbers in vivo. Iwano *et al.* designed a bioluminescence imaging system that produces brighter emission by up to a factor of 1000 compared with conventional technology (see the Perspective by Nasu and Campbell). Individual tumor cells were successfully visualized in the lungs of mice. Small numbers of striatal neurons were detected in the brains of naturally behaving marmosets. The ability of the substrate to cross the blood-brain barrier should provide important opportunities for neuroscience research.

Science, this issue p. 935; see also p. 868